

LNF-90/101

A. La Monaca, E. Burattini, G. Cappuccio, J.S. Shah, S. Simeoni, A. Stecchi,
L. Trasatti

**IMPROVED PERFORMANCE OF THE DRIFT-CHAMBER DETECTOR AT ADONE
WIGGLER**

Estratto da: Conf. Proc. Vol. 25 XSR-89, A. Balerna, E. Bernieri, S. Mobilio (Eds.)
SIF Bologna, Pag. 345 (1990)

IMPROVED PERFORMANCE OF THE DRIFT-CHAMBER DETECTOR AT ADONE WIGGLER

A. La Monaca^(*), E. Burattini ^(o), G. Cappuccio^(oo), J.S. Shah ^(**), S. Simeoni^(*), A. Stecchi^(*),
 L. Trasatti^(*)

- ^(*) INFN, Lab. Naz. di Frascati, 00044 Frascati, Italy
^(o) CNR, Lab. Naz. di Frascati, 00044 Frascati, Italy
^(oo) CNR, Ist. di Strut. Chim., 00016 Monterotondo Sc., Italy
^(**) H.H. Wills Physics Laboratory, University of Bristol, Bristol BS8 1TL U.K.

ABSTRACT

Improved performance of Drift-Chamber area gas detector, incorporating a CAMAC-VME-Macintosh Iix data acquisition system providing real time graphics, is reported. The detector was used with a new diffraction apparatus for small, medium and wide angle diffraction experiments at Frascati Synchrotron Radiation Facilities (FSRF). Preliminary applications of low angle diffraction experiments are described.

1. Introduction

X-ray Synchrotron Radiation sources offer a good opportunity to study, dynamically, structural changes occurring in materials of different types including biological materials. It is however desirable to use a radiation area detector, with a certain combination of properties [1,2,3], for mapping two dimensional distribution of the diffracted intensities in the plane of detection (because it genuinely gives information on the texture and the structure of the specimen, otherwise not possible).

Table I: Performance of the Drift-Chamber and the Diffraction Apparatus

Drift-Chamber:		
Quantum efficiency at $\lambda=1.54 \text{ \AA}$ and using Ar (Xe) mixtures	20 (84)	%
Detecting area	17 x 20	mm ²
Spatial resolution on the detector plane: X(drift) x Y(delay).	120 x 160	μm^2
Pixel number	142 x 125	pixels
Maximum storage of the buffer memories	256 x 256	pixels
Maximum counting rate for each pixel	2.2×10^4	cps
Maximum count capacity of detector	1×10^6	cps
Maximum linear count of the whole system	7×10^5	cps
Diffraction Apparatus:		
Diameter of pin-hole collimator (variable)	0.5	mm
Primary beam angular divergence : horizontal - vertical	76" - 6"	arcsec
Cross section of the beam at specimen: horizontalxvertical	0.68x0.51	mm ²
Intensity on the sample ($\lambda=1.54 \text{ \AA}$, $\Delta\lambda/\lambda=10^{-4}$, I =30 mA single bunch)	2.4×10^7	phot/sec
Conical angle of parasitic scattering	495"	arcsec
Specimen-detector distance: max. - min.	500 - 40	mm
Maximum angle obscured by the beam-stopper	227"	arcsec
Angular range covered by the detector at max. and min.distance	2° - 25°	deg
Angle range covered by the goniometer at max. and min. distance	25° - 134°	deg
Max. and min. angular resolution on the detector plane: X coord.	50" - 618"	arcsec
Max. and min. angular resolution on the detector plane: Y coord.	66" - 825"	arcsec

Ideally a good area detector should have: (1) a large area, (2) uniform sensitivity of detection, (3) a good quantum efficiency, (4) high count rate (per pixel), (5) wide dynamic range, (6) high temporal resolution, (7) high spatial resolution in every direction for the whole area of the detector, (8) non-deterioration of sensitivity and performance with time, (9) immunity from radiation damage and (10) capability of being interfaced to a real time data processing system.

Presently available area detectors, as gas avalanche discharge detectors and solid state detectors, do not have the ideal combination of the properties listed above. They suffer from several disadvantages [2,4], which have been only marginally improved by current technology and researches [5,6,7].

The principal disadvantages of gas detectors and solid state detectors (CCD and photodiodes) have been listed before [2,4]. Additionally for CCD detectors there is a presence of a certain "dead time" due to a long "total duration time of scintillation" for each absorption event. Also CCDs are "slow" because of only one readout channel for reading more than 10^5 pixels. Both gas and solid-state detectors have limited count rate because of low transmission rate of the data acquisition systems currently available.

However a gas detector can offer the following advantages: (1) it is possible to tailor it to a specific experiment to incorporate the desirable characteristics; (2) it can be more reliable.

Here we report some RECENT IMPROVEMENTS in the performances of the Frascati Drift-Chamber detector [2,8], using the ADONE Wiggler source, on a diffraction apparatus for small, medium and wide angle experiments and incorporating a new computerized ARGO system based on CAMAC-VME-Macintosh IIx. Finally, we show preliminary results on the low angle diffraction data on crimped collagen.

2. Drift-chamber area detector

Fig. 1. shows the experimental apparatus schematically. Table I lists new characteristics related to the improved performance of the detector. These are due to change in the geometry of the detector and utilization of the synchrotron radiation time structure.

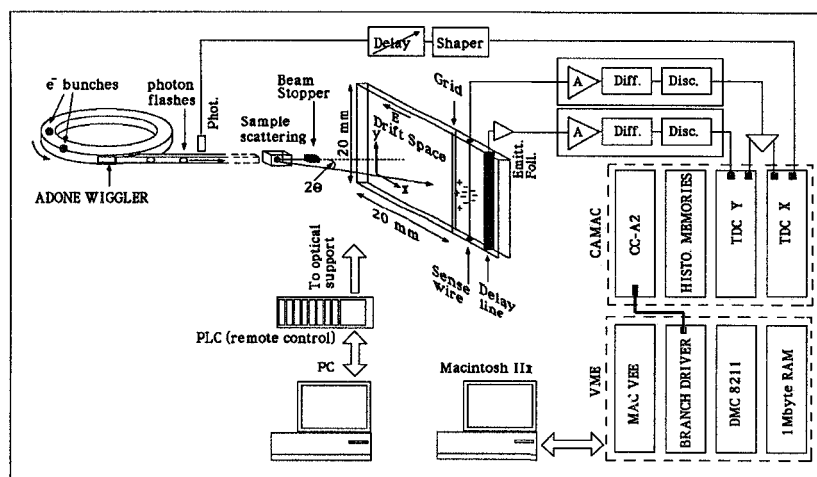


Fig. 1: Diagram of the drift-chamber area detector apparatus for diffraction.

The detector has : (a) no wire grid to produce a uniform electric potential detecting area, and (b) a small charge proportional gas gap region (2.5 mm), separated from the "drift region", where the high density of ion discharges avalanches can be easily collected by a semicylindrical cathode.

The mechanism of temporal operation of the detector has been described before [8]. Briefly, the X coordinate of the position of an impinging X-ray photon is detected by measuring the drift time $\Delta t = t_1 - t_0$ of the electronic cloud, generated in the gas by the photon, which drifts in the detection plane at constant velocity up to the anode wire (t_0 , is "the zero time" given by the time structure of the synchrotron radiation). To determine the Y coordinate a continuous delay line (11nsec/mm delay time), developed by us, is placed at a distance of 2.5 mm from the anode to detect the position of the avalanche discharge along the wire. The use of high speed electronic circuits has enabled us to obtain better resolution for both coordinates.

The detector is mounted on a goniometer.

3. ARGO system

The ARGO (Acquisition of data with Real time Graphic Output) system was designed by us to acquire real time user controlled graphics and data handling. It uses a Macintosh Ix computer to control CAMAC and the VME bus.

A pair of Le Croy model 4204 CAMAC TDC's (Time to Digital Converters), with conversion time of about 1 μ sec., have been used. To take full advantage of the speed of the chamber and of the TDC's, their output is immediately stored into two Le Croy 3588 Histogram Memories via a separate bus, independent of the CAMAC dataway. The Macintosh reads the contents of the histogram memories during data taking, displays the results graphically and saves them as appropriate. CAMAC commands also allow one to control TDC parameters and acquisition start-stop operations.

Communication to the Macintosh computer was via its own bus "Nubus", a MICRON interface board [9] through a MacVee controller and a CES CDB 8210 CAMAC Branch Driver together with a DMC 8211 DMA controller interfaced to the VME crate to CAMAC crate. A 1 Mbyte VME memory was used as VME buffer. The system has a capacity of 128x256 channels with a maximum of 65,536 counts per channel or 256x256 channels with a maximum of 4095 counts per channel, respectively.

The software for the system is in Real Time Fortran RTF, developed at CERN [10]. It is possible to view different graphic displays of the experimental data in real time. One dimensional projected intensity histograms (X or Y coordinate), two-dimensional pseudocolour plots, and two-dimensional intensity maps with the intensity displayed in the third dimension can be viewed. The 3 dimensional display uses a "2 vanishing points perspective" to give a good sense of depth without introducing any distortion in the vertical axis. Fig.2 shows such a plot for alcian blue stained collagen. The ARGO system is linear up to a counting rate of 700 KHz.

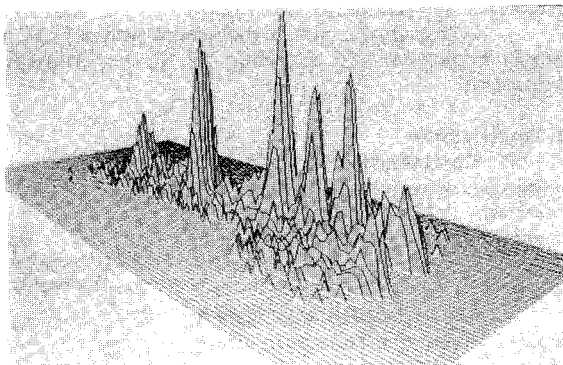


Fig. 2: Low angle diffraction pattern of alcian blue stained collagen. The beam stop is located along the axis of the main beam and in the figure is seen (as absence of any relief) before the occurrence of peaks which are along the meridional direction (i.e. the axis of the fibre).

4. Diffraction apparatus

Diffraction apparatus, shown in fig. 3, is on BX1 beam line of PWA laboratory at ADONE Wiggler source with monochromatic radiation, in the range of energy, 3-27 keV (including 1.54 Å. X-rays). The diffraction apparatus, has the same geometry used previously [11]. For obtaining diffraction patterns of mechanically stretched, hydrated biological specimens an additional environmental chamber incorporating a fully automatic miniature tensometer [12] can be inserted in between the drift chamber detector and the vacuum

chamber. The main vacuum specimen chamber contains micrometer movements for aligning the specimen. There is also a thermostatic cell to hold a specimen in the range of temperature -30/+150 °C. It is possible to change the specimen-detector distance to obtain small, medium and wide angle diffraction experiments on the same specimen because the detector is linked to the specimen chamber via a telescopic vacuum pipe.

Although Synchrotron Radiation beam is highly collimated, we use two pinhole combination^[11], to cut down parasitic scattering. Using pin-holes of diameters 0.3 and 0.5 mm, placed 500 mm apart a reduction of parasitic scattering of about two order of magnitude was achieved. A set of pin-holes in the range 0.1 - 1.2 mm of diameter have been fabricated in gold disks, in truncated conical shapes to avoid scattering at grazing angle. The holes can be aligned by the provision of micrometer screw movements.

The beam stop (2 mm width), is also made of gold and can be moved by remote control for alignment. It is placed on the entrance window of the detector. For alignment and location of the main beam it contains a of 0.1mm at its center. This can be blocked by a micro-shutter situated at the rear of the beam stop.

A fast remote control movement system (PLC Omron Sysmac C200H) for moving the whole apparatus and adjusting all the experimental parameters is available with the apparatus.

5. Applications

The drift-chamber diffraction apparatus was successfully used to confirm other measurements regarding the size, the apparent divergences and the stability of the wiggler source position.

The apparatus was used to study the presence of crimps in turkey tendon ^[12]. Crimping in collagenous tissues is fundamental to the biomechanical studies of the connective tissues. Crimping comprises a predominant arrangement of the fibrils in the tissues whereby the axes of the fibrils undulate in a well known zig-zag pattern. It is due to this that in the low angle diffraction pattern one should find reflections corresponding to at least two different directions.

Fig. 4a shows a low angle diffraction pattern of uncalcified and unstretched tendon collagen from turkey 20 weeks old. It clearly shows presence of crimping in turkey tendon. This is compared with the pattern

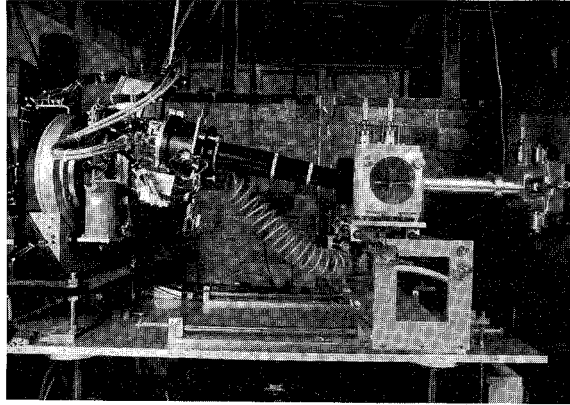


Fig. 3: Photograph of the diffraction apparatus with the drift-chamber area detector tilted to the axis of the X-ray beam.

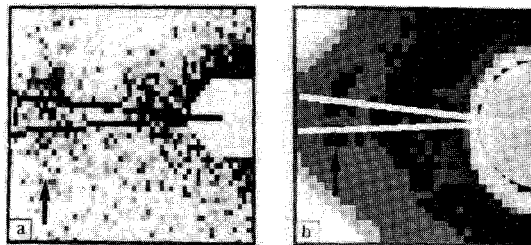


Fig. 4: Diffraction patterns of the crimped collagen fibres showing reflections occurring along at least two meridional directions:(a) drift chamber data of uncalcified and unstretched turkey tendon of 20 weeks old; (b) digitized film data of human palmaris longus tendon. The arrows show overlapping reflections in each pattern.

obtained by Nicholls et al on palmaris longus human tendon [13]. Fig. 4b shows a part of the colour coded pixel pattern from the digitized data of the original film (512X512 pixels). The azimuthal resolution of the data recorded by the drift chamber detector is as good as that obtained previously by the use of the film.

6. Conclusion

It is therefore concluded that the apparatus at Frascati is eminently suitable for studying the mechanical behavior of the crimped tissues for very important biomechanical functions and for designing soft tissue prostheses [14,15]. It is intended to use the apparatus for (1) further dynamic studies of mechanical behavior of crimping, (2) fractal structure occurring in kinetic processes of gels formation in silica, (3) weak scattered intensity profiles of polyamide fibers, polysaccharides solutions, or paramyosine structures.

It is proposed to improve further the performance of the drift chamber by employing CF_4 gas to utilize higher drift velocity and increasing the effective detecting area.

Acknowledgements

We are greatly indebted to Prof. A. Bigi, A. Ripamonti and N. Roveri of Bologna University for supplying us with samples and for helpful discussions. We like to thank Dr. A. Giovannella of L'Aquila University for his collaboration to the data processing. We acknowledge the constant personal attention to our project by the LNF director Prof. S. Tazzari. We wish to thank the Machine Division staff for providing special support for Adone single bunch operation, the mechanical SPECAS service and the photographic laboratory of the LNF for their assistance. We acknowledge financial help from the EEC (J.S. Shah). The development of the ARGO system was supported by Gruppo V of INFN under the FADD research grant.

References

- [1] N.A. Mesentsev et al., Nucl. Instr. and Meth. A246 (1986) 604.
- [2] A. La Monaca et al., BIOPHYSICS AND SYNCHROTRON RADIATION. Springer Series in Biophysics vol. 2 p.303. Ed. by A. Bianconi and A. Congiu-Castellano Springer and Verlag, Berlin 1987.
- [3] L. J. Gathercole and J. S. Shah, Int. J. Macromol. 9 (1987) 181.
- [4] A. La Monaca, Report INFN-LNF 87/70(R), 1987; and V.A.J. Van Lint, Nucl. Instr. and Meth. A253 (1987) 453; and V. Radeka, Nucl. Instr. and Meth. A253 (1987) 309.
- [5] A. Faruqi, Nucl. Instr. and Meth. A269 (1988) 362.
- [6] R. Lewis et al., Preprint Daresbury Laboratory DL/SCI/P568A.
- [7] ENRAF-NONIUS, Highview House, 165 Station Road, Edgware, Middlesex HA8 7JU.; and NICOLET INSTRUMENT CO., 5225 Verona Road, P.O. 4370, Madison WI. 53711-0370.
- [8] M. Iannuzzi and A. La Monaca, Nucl. Instr. and Meth. 201 (1982) 197.
- [9] B.G. Taylor: "The MacVEE Hardware User Manual". Rev. 4.1, CERN EP Division, 1987; and B.G. Taylor: "The MICRON User Manual". Rev 1.0, CERN Division, 1988.
- [10] H. von der Schmitt: "RTF/68K, Real-Time FORTRAN-77 for 68K Processors". Physikalisches Institut Universität Heidelberg CERN UA1, March 9, 1988; and MacUA1 and MacSYS are a Macintosh based development system developed at CERN in the UA1 experiment.
- [11] L. Allocca et al., Nucl. Instr. and Meth. 219 (1984) 227.
- [12] J.S. Shah et al., "A New Instrumentation for Mapping Structural and Textural Changes in Fibres with Stress by Wide and Low Angle Diffraction at Adone". These Proceedings.
- [13] Nicholls et al., Annals Rheum. Dis. 43(1984)477.
- [14] J.S. Shah, "Connective Tissue Prosthesis" U.S. Patent No 4,642,119 (1987); also U.K. & European Patents.
- [15] A. Ripamonti et al.: "Structural Organization of Macromolecular and Inorganic Components of Calcified Biological Tissues". Experimental Proposal to FSRF, Frascati 1988.